Glycoconj J (2006) 23: 135–141
DOI 10.1007/s10719-006-5446-8

Structural analysis of a designed inhibitor complexed with the hemagglutinin-neuraminidase of Newcastle disease virus

Charlotte Ryan · Viateslav Zaitsev · David J. Tindal · Jeffrey C. Dyason · Robin J. Thomson · Irina Alymova · Allen Portner · Mark von Itzstein · Garry Taylor

Abstract Viruses of the *Paramyxoviridae* family are the leading cause of respiratory disease in children. The human parainfluenza viruses (hPIV) are members of the *Paramyxovirinae* subfamily, which also includes mumps virus, Newcastle disease virus (NDV), Sendai virus (SV) and simian type 5 virus (SV5). On the surface of these viruses is the glycoprotein hemagglutinin-neuraminidase (HN), which is responsible for cell attachment, promotion of fusion and release of progeny virions. This multifunctional nature of HN makes it an attractive target for the development of inhibitors as a treatment for childhood respiratory diseases. Here we report the crystal structure of NDV HN in complex with a derivative of 2-deoxy-2,3-dehydro-*N*-acetylneuraminic acid, Neu5Ac2en, that has a functional group designed to occupy a large conserved binding pocket around the active site. The purpose of this study was to examine the effect of a bulky hydrophobic group at the O4 position of Neu5Ac2en, given the hydrophobic nature of the binding pocket. This derivative, with a benzyl group added to the O4 position of Neu5Ac2en, has an IC_{50} of $\sim$10 μM in a neuraminidase assay against hPIV3 HN. The IC_{50} value of the parent compound, Neu5Ac2en, in the same assay is $\sim$25 μM. These results highlight the striking difference between the influenza neuraminidase and paramyxovirus HN active sites, and provide a platform for the development of improved HN inhibitors.

Keywords Neuraminidase · Sialidase · Hemagglutinin-neuraminidase · Structure-based drug design · Newcastle disease virus · Parainfluenza

C. Ryan · V. Zaitsev · G. Taylor (✉)
Centre for Biomolecular Sciences, University of St Andrews, St Andrews, Fife, KY16 9ST, Scotland, UK
e-mail: glt2@st-andrews.ac.uk.
Tel: +44 1334 467301
Fax: +44 1334 462595

D. J. Tindal · J. C. Dyason · R. J. Thomson · M. von Itzstein
Institute for Glycomics, Griffith University, PMB 50 Gold Coast Mail Centre, Queensland 9726, Australia

I. Alymova · A. Portner
Department of Infectious Diseases, St. Jude Children's Research Hospital, Memphis, Tennessee 38105-2794, USA

Introduction

The family *Paramyxoviridae* is a large group of enveloped, non-segmented negative stranded RNA viruses that include many important human pathogens, such as human parainfluenza viruses (hPIV) serotypes 1–4, mumps virus, measles virus, and human respiratory syncytial viruses (RSV). As a group the hPIVs and RSV are the leading cause of respiratory diseases in children [1–3]. The family is divided into two subfamilies, *Paramyxovirinae* and *Pneumovirinae*. The subfamily *Paramyxovirinae* is composed of three genera: *Respirovirus*, *Rubulavirus*, and the *Morbillivirus*. Besides human viruses, these genera also include many animal viruses, whose structure, amino acid sequence and life cycle are highly similar to their corresponding human viruses. For example, the Respirovirus genus includes the human pathogen hPIV1 and the murine parainfluenza type 1 Sendai virus (SV). Rubulavirus genus includes mumps virus, the avian pathogen NDV and the simian type 5 virus (SV5, now reclassified as PIV5). Epidemiologically, parainfluenza viruses and RSV are responsible for annual epidemics, and reinfection in later years is common, although less severe [4]. Thus, immunity that develops through natural infection is not sufficient to provide complete protection. In infants and children, especially in the first six months of life,

parainfluenza viruses are the most important causes of croup (hPIV1) and serious causes of bronchiolitis and pneumonia (hPIV3) [1,3,4]. Effective virus vaccines are available for only mumps and measles viruses. Inactivated vaccines have been prepared against other parainfluenza viruses and RSV, but these vaccines have been ineffective [5].

The Respirovirus and Rubulavirus genera have two surface glycoproteins, the hemaggltuinin-neuraminidase (HN) and the fusion protein (F). HN has three functions: (i) it recognizes sialic acid containing receptors on cell surfaces, (ii) it promotes the fusion activity of the F protein allowing the virus to penetrate the cell surface, and (iii) it acts as a neuraminidase (sialidase), removing sialic acids from progeny virus particles to prevent viral self-agglutination thereby aiding viral spread [3]. As paramyxovirus neuraminidases have an acid optimum (pH 4.8 to 5.5), it is likely that the neuraminidase acts in the *trans* Golgi network, removing sialic acid from glycosylated HN and F proteins destined for the cell membrane [3]. Many studies show that only homotypic HN and F can induce fusion [6], suggesting that there is a specific interaction between HN and F, involving both the stalk and globular head regions of HN.

The first crystal structure of HN described was that of the catalytically-active head region (residues 124 to 569) of HN from the Kansas strain of Newcastle disease virus (NDV) [7]. The recent reports of the structures of hPIV3 HN and SV5 HN, both determined using the NDV HN structure as a search model, have confirmed a highly conserved monomer structure despite sequence identities as low as 25% [8,9]. In the crystal, NDV HN and SV5 HN form tight dimers, disulfide-linked in the case of SV5 HN, that can associate into tetramers [7,9] (Figure 1a). This is in agreement with electron microscope images of released HN molecules that show a mixture of dimers and tetramers [10]. The structural studies on NDV HN revealed two dramatically different forms of the HN dimer, and two distinct states of the catalytic site, suggesting a pliable site that could switch between being a sialic acid binding site and a catalytic site [7]. Subsequent mutagenesis studies supported this hypothesis: mutation of most of the amino acids in the site severely reduced neuraminidase activity, and also had a significant effect on hemagglutinin activity (an assay for sialic acid binding) and fusion activity [11]. Further mutagenesis studies on NDV HN also suggested that the dimer interface is involved in the fusion process [12,13]. The picture that emerged from these experiments is that the pliable active site and the dimer association may be involved in the promotion of fusion. A second sialic acid binding site was discovered at the dimer interface of NDV HN [14], but this may be unique to NDV [9]. The structural studies on SV5 HN have suggested an alternative model for triggering by HN of F into its fusogenic state, namely through changes in the tetrameric arrangement of HN induced upon binding sialic acid containing receptors.

HN is therefore an attractive target for inhibition, given the ability of each HN monomer to bind and hydrolyse sialic acid containing glycoconjugates via one sialic acid recognition site. When compared with the structures of other neuraminidases/sialdiases, HN has a uniquely large cavity around the O4 position of its substrate, which is lined with residues that are largely conserved across all HNs (Figure 1b). Using the structure of NDV HN in complex with Neu5Ac2en (**1**) as a starting point, derivatives of Neu5Ac2en with bulky groups in place of the O4 hydroxyl have been synthesised, which show efficacy against human parainfluenza viruses [15]. In these studies reverse genetics was used to engineer a modified Sendai virus carrying hPIV1 HN on its surface. The recombinant virus was lethal to mice, but pretreatment with these ligands 4 h before the start of infection afforded protection from death, thereby establishing the validity of HN as a drug target [15].

As part of an ongoing study to develop inhibitors of HN, we have synthesised derivatives of Neu5Ac2en with bulky ether-linked hydrophobic groups replacing the O4 hydroxyl group. Here we report the structure of NDV HN in complex with HN108 (**2**, 4-*O*-benzyl-Neu5Ac2en), where the bulkier aromatic group at O4 was designed to fill the HN cavity that is lined with hydrophobic and polar amino acids.

Materials and methods

Crystals of the globular ectodomain of NDV HN (residues 124–570) were obtained using the published conditions [16]. For NDV HN, reproducible, well diffracting crystals are readily formed at pH 4.6 for use in soaking experiments with inhibitors, and this crystal form (orthorhombic) was used in these studies. Two other crystal forms of NDV HN have been reported that are obtained by co-crysallisation with Neu5Ac2en [14,16], but obtaining these crystal forms with other ligands was not readily reproducible. The inhibitor HN108 (2-deoxy-2,3,-dehydro-4-*O*-benzyl-*N*-acetylneuraminic acid, 4-*O*-benzyl-Neu5Ac2en) as a lyophilised powder was resuspended in the mother liquor (15% PEG 4 K, 0.1 M citrate pH 4.5 and 0.2 M ammonium sulfate). The inhibitor was prepared and biologically evaluated against hPIV3 in our laboratories (von Itzstein, M., and Suzuki, Y. manuscript in review). Native NDV HN crystals were transferred to a 2 μl sitting drop containing 12.5% PEG 4 K, 0.1 M Na acetate trihydrate pH 4.6, 0.2 M ammonium sulfate and left to equilibrate for 4 h. HN108 was diluted in the mother liquor to a final concentration of 15 mM. Drops of the diluted compound were placed onto a siliconised cover slip and equilibrated to 4°C. Crystals were looped and placed in the 15 mM ligand drop for 20 min. All soaking experiments were performed at 4°C. Ligand-soaked crystals were transferred briefly to mother liquor containing 9.5% glycerol and

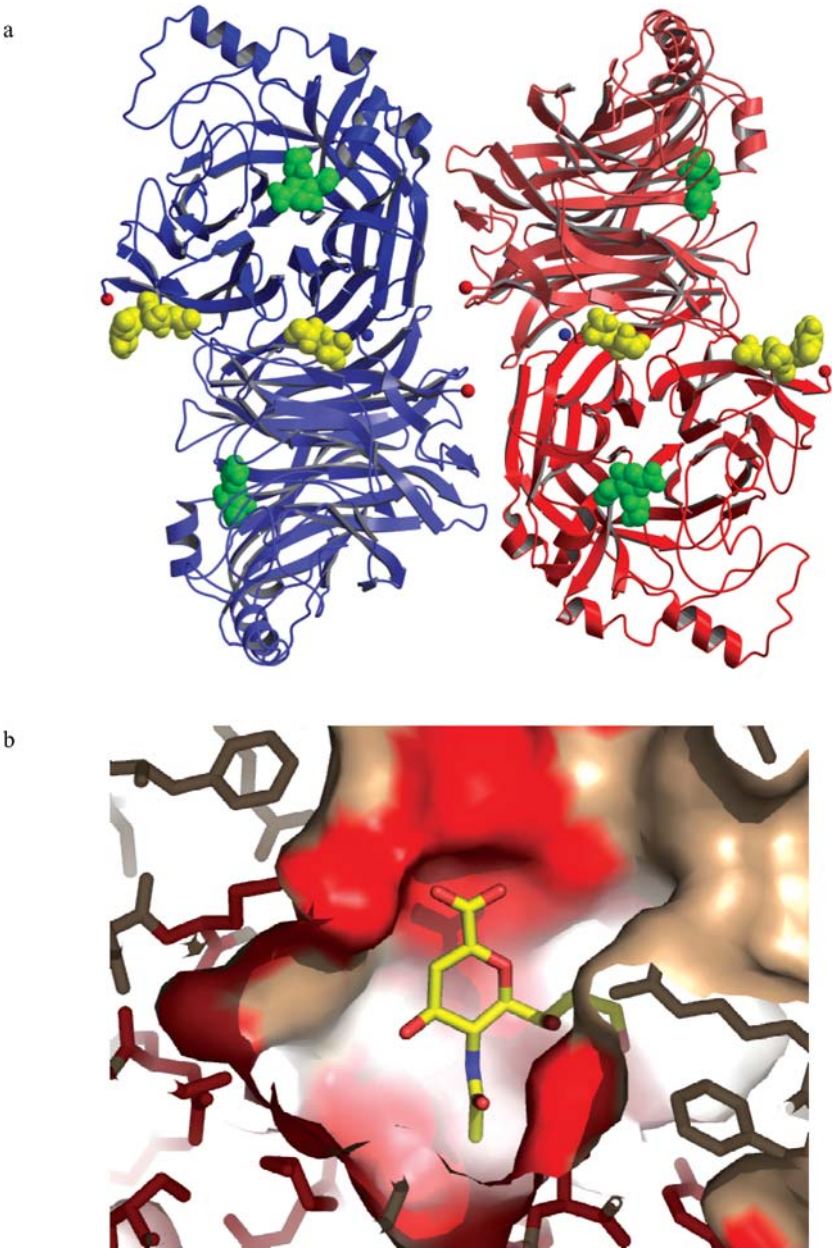

Fig. 1 NDV HN in complex with Neu5Ac2en. (a) The NDV HN tetramer with Neu5Ac2en (green) and Neu5Ac (yellow) bound. (b) Showing the large cavity around O4 of Neu5Ac2en, and the conserved nature of the sialic acid recognition or catalytic site, where the surface of the protein is coloured red for residues that are invariant across all paramyxovirus HNs.

then to mother liquor containing 19.5% glycerol. Crystals were incubated in the cryoprotectant for three minutes then looped and frozen with liquid nitrogen for data collection.

Data were collected at 100 K on the ESRF beamline ID14-3 equipped with a MAR CCD detector at a wavelength of 0.93 Å. Data collection statistics are given in Table 1. Diffraction data were integrated using MOSFLM [17] and scaled using SCALA from the CCP4 suite of programs [18]. NDV HN crystals suffer from extreme non-isomorphism, with large unit cell changes between crystals. Accordingly, molecular replacement was used with AMoRE to place the two HN monomers (search model 1E8U) in the asymmetric unit of the orthorhombic unit cell. CNS [19] was used to refine the model, with rounds of model building using O [20]. CNS was also used to automatically detect potential water molecules that were then checked by hand in O. The programs ProDrg [21] and Sybyl v6.6 (Tripos Inc.) were used to define ligand coordinates and generate their respective topology and parameter coordinate files.

Results

The orthorhombic crystal form of HN used in these studies has two molecules of NDV HN in the asymmetric unit. In the absence of ligand, or in the presence of the β-anomer of Neu5Ac, the sialic acid recognition site shows some major changes in the positions of certain conserved amino acids

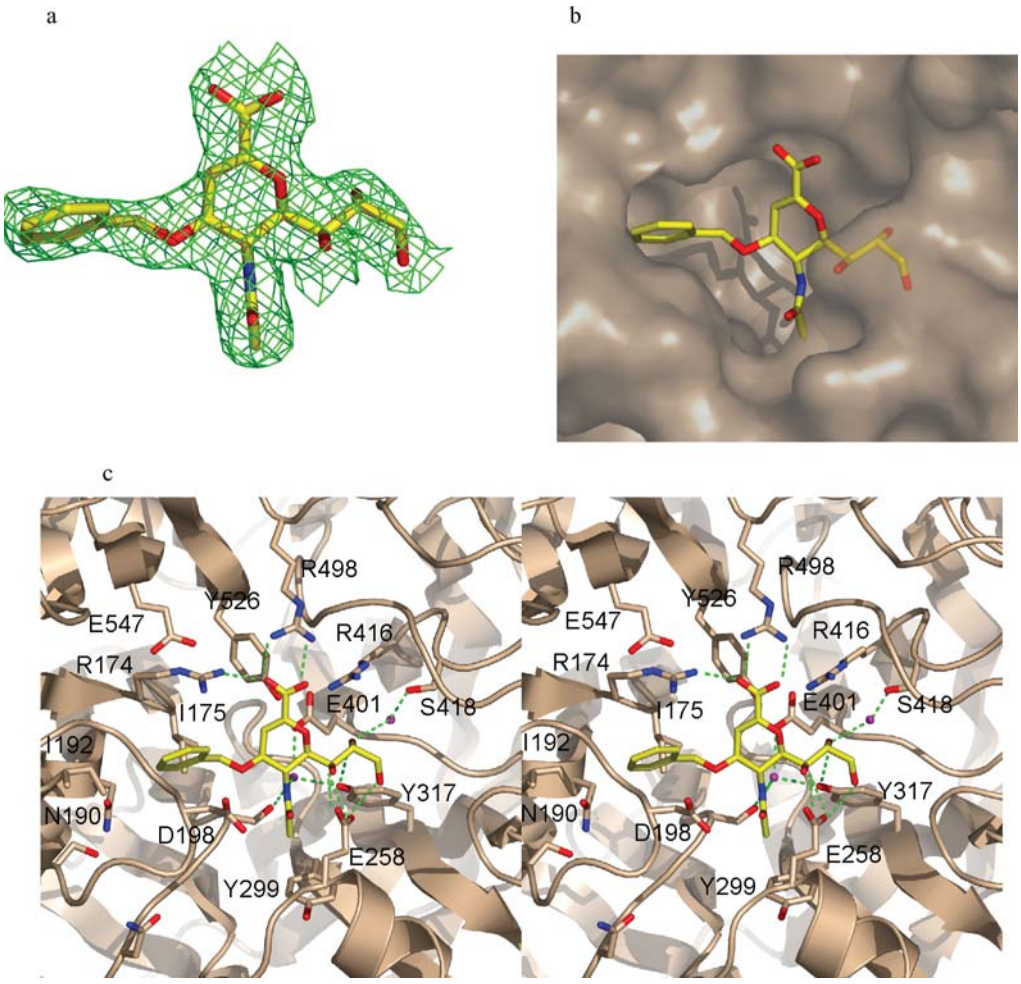

Fig. 2 NDV HN complexed with HN108 (4-*O*-benzyl-Neu5Ac2en, (2). (a) A 2FoFc map around the ligand, contoured at 1σ. (b) HN108 in the binding pocket. (c) Stereo view of the ligand interactions. Only direct hydrogen bonds made between HN108 and the protein are shown as dotted green lines. Two water molecules are drawn as magenta spheres.

suggesting a switch mechanism that allows the site to change from a sialic acid binding site (switched-off) to a catalytic site (switched-on) [7]. In the complex with HN108, monomer A reveals clear electron density for the ligand in the active site (Figure 2a and b), whereas monomer B shows little or no evidence of ligand. In addition, upon ligand binding, monomer A is converted into the structure observed in the complexes of NDV HN with Neu5Ac2en in the hexagonal and tetragonal crystal forms (switched-on), whereas monomer B remains in its switched-off state. There are major conformational changes between these two states which monomer A is able to undergo in the crystal, whereas monomer B is constrained by crystal packing and remains in its switched-off state. The following discussion will focus on monomer A.

The carboxylate, glycerol and *N*-acetyl groups of HN108 make the same interactions with NDV HN as observed in the Neu5Ac2en complex [7] (Table 2, Figure 2c). Arg 174 is stabilised by interactions with Glu 547. When superimposed onto the Neu5Ac2en-HN structure (PDB code 1E8V), Tyr 526 is positioned in the catalytic orientation with its hydroxyl group close to the C1─C2 bond of HN108. Lys 236 is also in the 'active'-state position i.e. swung into the cavity previously occupied by Arg 174. The amido N of the *N*-acetyl group interacts with Ser 237, Tyr 317 and Glu 401 via a water molecule in a manner similar to that described for the Neu5Ac2en-HN complex [7]. The glycerol group forms hydrogen bonds with Tyr 317, Glu 258 and Tyr 262 and interacts with Ser 418 via a water molecule. An additional interaction between Arg 416 and the hydroxyl group at position C8 is also seen.

The benzyl ring at the C4 position sits in the large pocket (Figure 2b), the plane of the ring sandwiched between the methylene side groups of Asp 198 and Arg 174, and making a number of non-bonded interactions predominantly with Ile 175 and Ile 192. Ile 192 and Asp 198 are conserved across all HNs, while Ile 175 is an threonine in hPIV3 HN, a leucine in hPIV1 HN and Sendai HN, but is otherwise conserved. Superimposing the structures of NDV HN, SV5

Table 1 Crystallographic data collection and refinement statistics. Values in parenthesis are for the highest resolution shell

	HN108
$P2_12_12_1$ unit cell (Å)	
a	73.23
b	77.21
c	202.72
Resolution range (Å)	50–2.8
Observed reflections	558,220
Unique reflections	32,019
Mosaicity (°)	0.67
Completeness (%)	88.1 (87.4)
$^*R_{merge}$ (%)	9.2 (31.3)
$<I/\sigma I>$	6.1 (2.4)
Refinement	
Reflections in working set	32,019
Reflections in test set	3,100
R-factor	0.228
R-free	0.271
Number of atoms	
Protein	6892
Waters	222
Ligand	50
Average B-factors (Å^2)	
Monomer A	40.0
Monomer B	
Waters	34.2
Ligand	47.9
rms deviations from ideality	
Bond lengths (Å)	.015
Bond angles (°)	1.87

$^*R_{\text{merge}} = \sum \|(k) - < | > |/ \sum |(k)$.

HN and hPIV3 HN shows the cavity to be highly conserved in structure. The only difference is the threonine in hPIV3 HN (position 193) at the position of Ile 175 in NDV HN. In hPIV3 HN, the methyl group of Thr 193 points towards C4 of Neu5Ac2en (PDB code 1v3d), maintaining a hydrophobic character to this part of the cavity. In the HN108 complex, Ile 175 has rotated about 180° around its $\chi 2$ torsion angle compared to the Neu5Ac2en-HN or apoprotein structures, to make a more favourable interaction with C12 of HN108. Finally, a water molecule that is observed interacting with O4 in all three viral HN-Neu5Ac2en complex structures, is displaced by the benzyl group of HN108.

1. Discussion

The sialic acid recognition site of HN serves three functions: to bind sialic acid receptors as the initial step of infection, to effect a conformational change in the fusion protein at the cell surface to initiate fusion, and to hydrolyse the release of sialic acids from progeny virus particles permitting viral spread. The multifunctional nature of the HN sialic acid recognition site makes it an attractive target for the development of specific inhibitors as treatments for childhood respiratory disease. When compared to the influenza virus neuraminidase, and neuraminidases from bacteria, parasites and mammals [22], the HN catalytic site is unusual in having a large cavity around the O4 position of sialic acid. This cavity is largely conserved across all paramyxovirus HNs, despite a large sequence variation across the viruses, suggesting that it must play some role in the function of HN. In the case of NDV HN, it has been argued that this conserved cavity is required to effect conformational changes associated with promotion of fusion upon binding sialic acid receptors [14].

The success of the development of chemical variants of Neu5Ac2en targeted to the influenza neuraminidase active site as drugs for the treatment of influenza, encouraged us to follow a similar strategy for HN. Zanamivir, or Relenza ®, a neuraminidase-based influenza drug, was developed by structure-based drug design, when it was predicted that substituting O4 of Neu5Ac2en with a positively charged group could fill a small cavity around O4 that was lined with two conserved glutamates [23]. For HN, the same strategy has been taken, namely to substitute Neu5Ac2en at the C4 position with groups that would, both in shape and charge character, complement the large cavity. This conserved cavity is lined with several hydrophobic groups: the side chains of two isoleucines (175 and 192 in NDV HN numbering) and the methylene groups of a conserved aspartic acid (198) and arginine (174). Although Ile 175 is not conserved across paramyxovirus HNs, it is substituted by either a leucine or threonine, preserving a hydrophobic characteristic. Ile 192 is conserved across all HNs. The cavity is also lined with polar main chain groups and the side chain of conserved residue Asn 190.

Two Neu5Ac2en derivatives have been previously reported, BCX2798 and BCX2855, which are promising leads with IC_{50}'s in the micromolar or sub-micromolar region for both neuraminidase and hemagglutinin assays against a range of HNs [15]. In addition, BCX2798 shows good efficacy in a mouse model of parainfluenza, thereby validating HN as a target for drug development. BCX2798 has an azide group in place of O4, and BCX2855 has a dichloromethanesulfonylamino group in place of O4. Both ligands also have an isopropyl group in place of the methyl group of the acetamido moiety of Neu5Ac2en. HN108 has an IC_{50} of ~10 μM in a neuraminidase assay against hPIV3, compared to

Table 2 Details of interactions of HN108 and NDV HN including interactions between water molecules trapped in the active site and coordinated by both protein and ligand

Hydrogen bonding			Non-bonding interactions		
HN108 atom	NDV HN atom	Distance (Å)	HN108 atom	NDV HN atom	Distance (Å)
		Carboxylate group			
O1A	Arg 174-N$^{\eta 2}$	2.64	C1	Arg 498 N$^{\eta 1}$	3.41
O1B	Arg 416 N$^{\eta 2}$	3.36	C1	Arg 498 N$^{\eta 2}$	3.36
O1A	Arg 498 N$^{\eta 1}$	2.70	C1	Tyr 526 O$^{\eta}$	3.43
O1A	Arg 498 N$^{\eta 2}$	3.39	O1A	Arg 498 C$^{\zeta}$	3.48
O1B	Arg 498 N$^{\eta 1}$	3.26	O1A	Tyr 526 C$^{\eta 1}$	3.33
O1B	Arg498 N$^{\eta 2}$	2.58	O1B	Arg 498 C$^{\zeta}$	3.28
		N-acetyl group			
N	Ser 237 O$^{\gamma}$	3.09	C10	Glu 258 O$^{\eta 2}$	3.55
	via H_2O	2.77			
N	Tyr 317 O$^{\eta}$	2.60	O10	Glu 258 C$^{\delta}$	3.16
	via H_2O	2.77			
N	Glu 401 O$^{\eta 2}$	2.76	O10	Lys 236 C$^{\eta}$	3.56
	via H_2O	2.77			
			C11	Tyr 299 C$^{\delta 2}$	3.55
			C11	Tyr 299 C$^{\eta 2}$	3.58
		Hydroxyl group			
O8	Arg 416 N$^{\eta 1}$	3.29	C7	Glu 258 O$^{\eta 2}$	3.17
O8	Tyr 317 O$^{\eta}$	3.07	O7	Glu 258 C$^{\delta}$	3.04
O9	Glu 258 O$^{\eta 2}$	2.86	C9	Glu 258 O$^{\eta 2}$	3.57
O7	Glu 258 O$^{\eta 1}$	2.50	O9	Thy 317 C$^{\eta 2}$	3.37
O7	Glu 258 O$^{\eta 2}$	2.88			
O9	Tyr 262 O$^{\eta}$	3.40			
O8	Ser 418 O$^{\gamma}$	2.30			
	via H_2O	2.86			
		Substituted aryl group			
			C12	Ile 175 C$^{\gamma 1}$	3.42
			C12	Ile 175 C$^{\delta 1}$	3.20
			C13	Ile 175 C$^{\gamma 1}$	3.96
			C13	Ile 175 C$^{\delta 1}$	3.75
			C14	Ile 175 C$^{\gamma 1}$	3.73
			C14	Ile 175 C$^{\delta 1}$	3.34
			C15	Ile 192 C$^{\delta 1}$	3.53
			C16	Ile 192 C$^{\gamma 1}$	3.89
			C16	Cys 196 O	3.30
			C16	Cys 196 C	3.93
			C16	Arg 197 C	3.76
			C16	Asp 198 C$^{\alpha}$	3.43
			C16	Asp 198 C$^{\beta}$	3.87
			C16	Asp 198 N	3.32
			C17	Arg 174 N$^{\eta}$	3.57
			C17	Asp 198 C$^{\alpha}$	3.64
			C17	Asp 198 C$^{\beta}$	3.56
			C17	Asp 198 N	3.43
			C18	Asp 198 C$^{\beta}$	3.76

$\sim$25 μM for Neu5Ac2en in the same assay (von Itzstein and Suzuki, manuscript under review). This encouraging result shows that the strategy of filling the cavity with a hydrophobic group should be explored further, perhaps by exploiting interactions with other features of the conserved cavity such as Asn 190.

Acknowledgments This work was supported by the Wellcome Trust and by the Engineering and Physical Sciences Research Council (EPSRC), who provided a studentship for CR. Staff of the European Synchrotron Radiation Facility (ESRF) are thanked for support in X-ray data collection. MvI gratefully acknowledges the support of the Australian Research Council (ARC) for the award of a Federation Fellowship.

References

1. McIntosh, K., Fishaut, M.: Immunopathologic mechanisms in lower respiratory tract disease of infants due to respiratory syncytial virus. Prog in Medical Virology **26**, 94–118 (1980)
2. Delage, G., Brochu, P., Pelletier, M., Gasmin, G., Lapoint, N.: Giant-cell pneumonia caused by parainfluenza virus. J. Pediatr. **94**, 426–9 (1979)
3. Lamb, R.A., Kolakofsky, D.: Paramyxoviridae: The viruses and their replication Fields Virology edited by Knipe, D., Howley, P.M. (Lippincott Williams & Wilkins, Philadelphia, USA, 2001) pp. 1305–40
4. Jackson, G.G., Muldoon, R.L.: Enteroviruses and paramyxoviruses, The University of Chicago Press, Chicago, 1975
5. Choppin, P.W., Scheid, A.: The role of viral glycoproteins in adsorption, penetration and pathogenicity of viruses. Rev. Infect. Dis. **2**, 40–61 (1980)
6. Hu, X.L., Ray, R., Compans, R.W.: Functional Interactions Between the Fusion Protein and Hemagglutinin—Neuraminidase of Human Parainfluenza Viruses. Journal of Virology **66**, 1528–34 (1992)
7. Crennell, S., Takimoto, T., Portner, A., Taylor, G.: Crystal structure of the multifunctional paramyxovirus hemagglutinin-neuraminidase. Nature Structural Biology **7**, 1068–74 (2000)
8. Lawrence, M.C., Borg, N.A., Streltsov, V.A., Pilling, P.A., Epa, V.C., Varghese, J.N., McKimm-Breschkin, J.L., Colman, P.M.: Structure of the haemagglutinin-neuraminidase from human parainfluenza virus type III. J. Mol. Biol. **335**, 1343–57 (2004)
9. Yuan, P., Thompson, T.B., Wurzburg, B.A., Paterson, R.G., Lamb, R.A., Jardetzky, T.S.: Structural studies of the parainfluenza virus 5 hemagglutinin-neuraminidase tetramer in complex with its receptor, sialyllactose. Structure (Camb.) **13**, 803–15 (2005)
10. Thompson, S.D., Laver, W.G., Murti, K.G., Portner, A.: Isolation of a Biologically-Active Soluble Form of the Hemagglutinin—Neuraminidase Protein of Sendai Virus. Journal of Virology **62**, 4653–60 (1988)
11. Connaris, H., Takimoto, T., Russell R., Crennell, S., Moustafa, I., Portner, A., Taylor, G.: Probing the sialic acid binding site of the hemagglutinin-neuraminidase of Newcastle disease virus: Identification of key amino acids involved in cell binding, catalysis, and fusion. *J. Virol* **76**, 1816–24 (2002)
12. Takimoto, T., Taylor, G.L., Connaris, H.C., Crennell, S.J., Portner, A.: Role of the hemagglutinin-neuraminidase protein in the mechanism of paramyxovirus-cell membrane fusion. J. Virol **76**, 13028–33 (2002)
13. Corey, E.A., Mirza, A.M., Levandowsky, E., Iorio, R.M.: Fusion deficiency induced by mutations at the dimer interface in the Newcastle disease virus hemagglutinin-neuraminidase is due to a temperature-dependent defect in receptor binding. J. Virol **77**, 6913–22 (2003)
14. Zaitsev, V., von Itzstein, M., Groves, D.R., Kiefel, M.J., Takimoto, T., Portner, A., Taylor, G.: Second Sialic Acid Binding Site in Newcastle Disease Virus Hemagglutinin-Neuraminidase: Implications for Fusion. J. Virol **78**, 3733–41 (2004)
15. Alymova, I.V., Taylor, G., Takimoto, T., Babu, Y.S., Chenghong, L., Xiaoping, X., Portner, A.: Efficacy of novel hemagglutinin-neuraminidase inhibitors BCX 2798 and BCX 2855 against human parainfluenza viruses *in vitro* and *in vivo*. Antimicrob Agents Chemother **48**, (2004)
16. Takimoto, T., Taylor, G.L., Crennell, S.J., Scroggs, R.A., Portner, A.: Crystallization of Newcastle Disease Virus Hemagglutinin-Neuraminidase Glycoprotein. Virology **270**, 208–14 (2000)
17. Leslie, A.G.W.: Recent changes to the MOSFLM package for processing film and image plate data. Joint CCP4 + ESF-EAMCB Bewsletter on Protein Crystallography, **26**, (1992)
18. CCP4. The CCP4 suite: Programs for protein crystallography. Acta Crystallographica D **50**, 760–763 (1994)
19. Brunger, A.T., Adams, P.D., *et al.*: Crystallography and NMR system: A new software suite for macromolecular structure determination. Acta Crystallographica Section D **54**, 905–21 (1998)
20. Jones, A.T., Zhou, J.Y., Cowan, S.W., Kjeldgaard, M.: Improved methodsfor the building of protein models in electron desnity mps and the location of errors in these models. Acta. Crystallographica A **47**, 110–19 (1991)
21. Schuttelkopf, A.W., van Aalten, D.M.: PRODRG: A tool for high-throughput crystallography of protein-ligand complexes. Acta. Crystallogr. D Biol. Crystallogr. **60**, 1355–63 (2004)
22. Taylor, G.: Sialidases: Structures, biological significance and therapeutic potential. Current Opinion in Structural Biology **6**, 830–37 (1996)
23. von Itzstein, M., Wu, W.Y., Kok, G.B., Pegg, M.S., Dyason, J.C., Jin, B., Phan, T.V., Smythe, M.L., White, H.F., Oliver, S.W., Colman, P.M., Varghese, J.N., Ryan, D.M., Woods, J.M., Bethell, R.C., Hotham, V.J., Cameron, J.M., Penn, C.R.: Rational design of potent sialidase-based inhibitors of influenza-virus replication. Nature **363**, 418–23 (1993)